

Adaptive Sliding Mode Control for an Active Gravity Offload System

Jiao Jia, Yingmin Jia and Shihao Sun

1 Introduction

Various methods of reducing gravity have been used such as parabolic flight, air-bearing, neutral buoyancy and suspension system [1–5]. These methods may be beneficial in some ways but are limited in others. Among them the suspension method [5–7] is superior on practicality, economy and reliability. There are two types of suspension methods passive suspension [5] and active suspension [6, 7]. The active suspension gravity offload method performs much better than the passive one. The offload accuracy of the active suspended system depends on the mechanical structure and the controller. Generally, a wire rope is one necessary part of the upright subsystem. However, the rope is flexible and easy to swing. To solve this problem, a buffer is developed. Besides, a creative suspension structure is developed to insure the object to rotate freely. The dynamic model of the system is deduced based on Lagrange equation. It's a nonlinear coupling system with disturbances, uncertainties and control input uncertainties. To ensure the system robust stability, an adaptive sliding mode controller is developed [8, 9].

2 Active Gravity Offload System (AGOS)

The AGOS is a servo platform consisting of a suspension structure, a buffer, a universal joint, a gantry robot, a tilt sensor, a tension sensor. The work flow chart is presented in Fig. 1. The specific connection relationship is shown in Fig. 2. The

J. Jia · Y. Jia (✉) · S. Sun

The Seventh Research Division and the Center for Information and Control,
School of Automation Science and Electrical Engineering,
Beihang University (BUAA), Beijing 100191, China
e-mail: ymjia@buaa.edu.cn

© Springer Nature Singapore Pte Ltd. 2018

Z. Deng (ed.), *Proceedings of 2017 Chinese Intelligent Automation Conference*,
Lecture Notes in Electrical Engineering 458,
https://doi.org/10.1007/978-981-10-6445-6_61

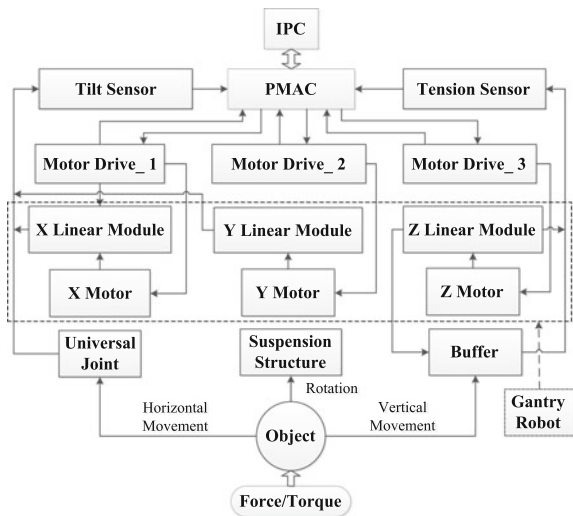


Fig. 1 The work flow chart

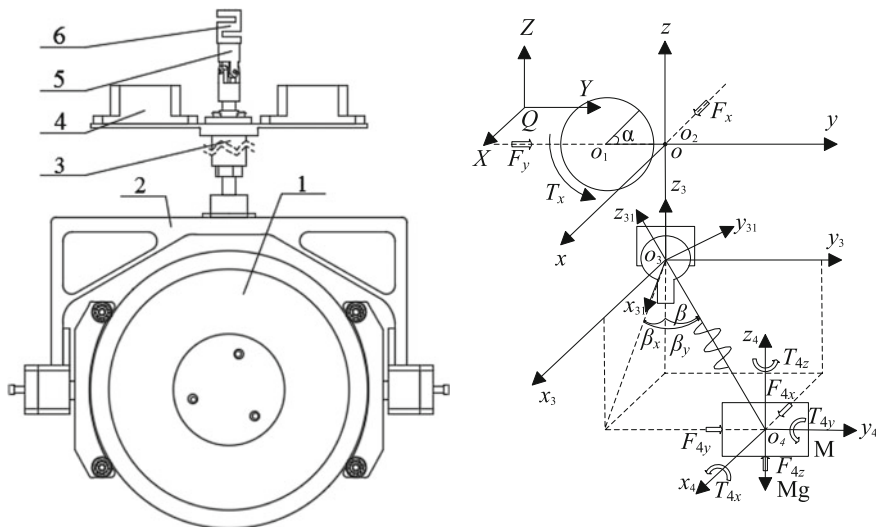


Fig. 2 The connection relationship and the coordinate system of AGOS. 1 object, 2 suspension structure, 3 buffer, 4 tilt sensor, 5 universal joint, 6 tension sensor

suspension structure is composed of rolling bearings and the corresponding fixations, which guarantees the equivalent suspension point to coincide with the centroid of the object. Hence, the object can maintain balance at any attitude.

According to Figs. 1 and 2, when the object is driven to move along the horizontal plane, the buffer swings around the universal joint and the tilt sensor can measure the swing angles. Then the X and Y linear modules will be driven by the X motor and Y motor to eliminate the swing angle to maintain the buffer vertically. When the object is driven to move vertically, the tension sensor will detect the variation of the buffer and then the Z linear module will be actuated by the Z motor to eliminate the variation as required. The control inputs are determined by the PMAC and the IPC. Then the variable gravity field is built for the object.

The AGOS coordinate system is shown in Fig. 2. The buffer is equivalent to a spring and the suspension structure is equivalent to a rope linked to the centroid of the object. The meaning of each part is as below.

- m_{0x}, m_{0y} , the load of X motor and the load of Y motor respectively,
- m_1, m_2 , the pinion and the rack mass,
- M , the object mass,
- α , the pinion rotation angle
- $Q - XYZ$, the static coordinate system
- O, m_{0x} centroid
- O_1, O_2, O_4 , centroids of m_1, m_2, M respectively,
- O_3 , the universal joint centroid,
- F_x, F_y , X motor and Y motor equivalent driven force on X and Y linear modules
- T_x , Z motor output torque on the pinion
- F_{4x}, F_{4y}, F_{4z} , the object driven force
- T_{4x}, T_{4y}, T_{4z} , the object driven torque
- β , swing angle between spring buffer and upright
- β_x, β_y , orthogonal decomposition of β
- $O - xyz$, coordinate moves with O ,
- $O_i - x_i y_i z_i, i = 3, 4$, coordinates move with O_3 and O_4 ,
- $O_3 - x_{31} y_{31} z_{31}$, coordinate rotates with the buffer.

According to the definition above, the coordinates of O, O_1, O_2 are $(x, y, 0)$, $(x, y - R, 0)$ and $(x, y, \alpha R)$ respectively.

The velocities of O, O_1, O_2 are $(\dot{x}, \dot{y}, 0)$, $(\dot{x}, \dot{y}, 0)$ and $(\dot{x}, \dot{y}, \dot{\alpha}R)$ respectively.

Denote $l_1 = Mg/k, d = l_0 + l_1 + l$ where l_0 is the free length of the spring. And O_4 is $(x + d \sin \beta_x \cos \beta_y, y + d \sin \beta_y, \alpha R - 0.5h_0 - d \cos \beta_x \cos \beta_y)$ where h_0 presents the length of the rack. O and O_2 are coincident at the initial position. The variation of the spring length is denoted by l . Define $l = 0$, when spring force is equal to the object.

When $\beta \leq 5^\circ$, let $\sin \beta \approx \beta, \cos \beta \approx 1$. The position and velocity of O_4 are

$$(x + d\beta_x, y + d\beta_y, \alpha R - 0.5h_0 - d), \left(\dot{x} + \dot{l}\beta_x + d\dot{\beta}_x, \dot{y} + \dot{l}\beta_y + d\dot{\beta}_y, \dot{\alpha}R - \dot{l} \right)$$

The object attitudes will be changed along with T_{4x}, T_{4y}, T_{4z} , and therefore the angular velocity is time-varying. But when x, y, α, l, β_x and β_y are choose as the system generalized coordinates, they are independent of the object rotational kinetic energy. Hence, when we calculate the system kinetic energy the object rotational kinetic energy could be ignored.

The system kinetic energy is

$$T = 0.5(0.5m_1R^2)\dot{\alpha}^2 + 0.5m_2(\dot{\alpha}R)^2 + 0.5m_{0x}v_{m0x}^2 + 0.5m_{0y}v_{m0y}^2 + 0.5M(v_{Mx}^2 + v_{My}^2 + v_{Mz}^2)$$

The pinion and rack move with the X and Y linear modules at the horizontal plane, so their kinetic energy is included in $0.5m_{0x}v_{m0x}^2 + 0.5m_{0y}v_{m0y}^2$.

Choose xOy plane as zero potential energy surface. Then the system potential energy is

$$V = m_2g\alpha R + 0.5k(l + l_1)^2 + Mg(\alpha R - 0.5h_0 - d)$$

$$L = T - V \quad (1)$$

The Lagrange equation

$$\frac{d}{dt} \left(\frac{\partial L}{\partial \dot{q}} \right) - \frac{\partial L}{\partial q} = Q_j \quad (j = 1, 2, \dots) \quad (2)$$

Substitute Eq. (1) into Eq. (2) and define $m = 0.5m_1 + m_2 + M, \eta_x = (M + m_{0x})/M, \eta_y = (M + m_{0y})/M, \eta = m/M, \varsigma = k/M, \eta_2 = (m_2 + M)/M, \rho = 1/M, \beta^2 = \beta_x^2 + \beta_y^2, \beta_x^y = \beta_x\dot{\beta}_x + \beta_y\dot{\beta}_y, \mathbf{q}_1 = [x, y, \alpha]^T, \mathbf{q}_2 = [l, \beta_x, \beta_y]^T$. We get

$$\mathbf{M}_1\ddot{\mathbf{q}}_1 + \mathbf{M}_2\ddot{\mathbf{q}}_2 + \mathbf{C}_1\dot{\mathbf{q}}_1 + \mathbf{C}_2\dot{\mathbf{q}}_2 + \mathbf{G}_1 = \mathbf{F}_1 \quad (3)$$

$$\mathbf{M}_2^T\ddot{\mathbf{q}}_1 + \mathbf{M}_3\ddot{\mathbf{q}}_2 + \mathbf{C}_3\dot{\mathbf{q}}_1 + \mathbf{C}_4\dot{\mathbf{q}}_2 + \mathbf{G}_2 = \mathbf{F}_2 \quad (4)$$

Obviously, M_2 is invertible as follow

Let Eq. (3) $-M_1M_2^{-T}$ Eq. (4) and because of $C_1 = C_3 = 0$ we gain Eq. (5)

$$\mathbf{M}_m(\mathbf{q}, \dot{\mathbf{q}})\ddot{\mathbf{q}}_2 + \mathbf{C}(\mathbf{q}, \dot{\mathbf{q}})\dot{\mathbf{q}}_2 + \mathbf{G}(\mathbf{q}) = \mathbf{F}_1 - \mathbf{M}_1\mathbf{M}_2^{-T}\mathbf{F}_2 \quad (5)$$

$$\mathbf{M}_m = \mathbf{M}_2 - \mathbf{M}_1\mathbf{M}_2^{-T}\mathbf{M}_3, \mathbf{C} = \mathbf{C}_2 - \mathbf{M}_1\mathbf{M}_2^{-T}\mathbf{C}_4, \mathbf{G} = \mathbf{G}_1 - \mathbf{M}_1\mathbf{M}_2^{-T}\mathbf{G}_2$$

$$\begin{aligned}
\mathbf{M}_1 &= \begin{bmatrix} \eta_x & 0 & 0 \\ 0 & \eta_y & 0 \\ 0 & 0 & \eta R^2 \end{bmatrix}, \mathbf{M}_2 = \begin{bmatrix} \beta_x & d & 0 \\ \beta_y & 0 & d \\ -R & 0 & 0 \end{bmatrix}, \mathbf{M}_3 = \begin{bmatrix} \beta^2 + 1 & d\beta_x & d\beta_y \\ d\beta_x & d^2 & 0 \\ d\beta_y & 0 & d^2 \end{bmatrix}, \mathbf{F}_1 \\
&= \begin{bmatrix} F_x \\ F_y \\ T_x \end{bmatrix} \\
\mathbf{C}_2 &= \begin{bmatrix} 2\dot{\beta}_x & 0 & 0 \\ 2\dot{\beta}_y & 0 & 0 \\ 0 & 0 & 0 \end{bmatrix}, \mathbf{C}_4 = \begin{bmatrix} 2\beta_x^y & 0 & 0 \\ 2d\dot{\beta}_x & 0 & 0 \\ 2d\dot{\beta}_y & 0 & 0 \end{bmatrix}, \mathbf{G}_1 = \begin{bmatrix} 0 \\ 0 \\ \eta_2 g R \end{bmatrix}, \mathbf{G}_2 = \begin{bmatrix} \zeta l \\ 0 \\ 0 \end{bmatrix}, \mathbf{F}_2 \\
&= \begin{bmatrix} F_{4z} \\ F_{4x} \\ F_{4y} \end{bmatrix}
\end{aligned}$$

3 Adaptive Sliding Mode Controller

For Eq. (5), define $\mathbf{M}(\mathbf{q}, \dot{\mathbf{q}}) = \mathbf{M}_m$, $\mathbf{F} = \mathbf{F}_1$, $\mathbf{F}_d = -\mathbf{M}_1 \mathbf{M}_2^{-T} \mathbf{F}_2$, and we obtain

$$\mathbf{M}(\mathbf{q}, \dot{\mathbf{q}}) \ddot{\mathbf{q}} + \mathbf{C}(\mathbf{q}, \dot{\mathbf{q}}) \dot{\mathbf{q}} + \mathbf{G}(\mathbf{q}) = \mathbf{F} + \mathbf{F}_d \quad (6)$$

Then $\ddot{\mathbf{q}}_2 = \mathbf{M}^{-1}(\mathbf{F} + \mathbf{F}_d - \mathbf{C}\dot{\mathbf{q}} - \mathbf{G})$. Define $\mathbf{x}_1 = \mathbf{q}_2 = \mathbf{q}$, we gain $\dot{\mathbf{x}}_1 = \mathbf{x}_2$, $\dot{\mathbf{x}}_2 = \mathbf{M}^{-1} \times (\mathbf{F} + \mathbf{F}_d - \mathbf{C}\dot{\mathbf{q}} - \mathbf{G})$. Define $\dot{\mathbf{x}} = [\dot{\mathbf{x}}_1, \dot{\mathbf{x}}_2]^T$, $\mathbf{u} = \mathbf{F}_1 = \mathbf{F}$, we gain Eq. (7)

$$\dot{\mathbf{x}} = \mathbf{f}(\mathbf{x}) + \mathbf{b}(\mathbf{x})\mathbf{u} + \mathbf{d} \quad (7)$$

where $\mathbf{f}(\mathbf{x}) = [\mathbf{x}_2, \mathbf{M}_m^{-1}(-\mathbf{C}\mathbf{x}_2 - \mathbf{G})]^T$, $\mathbf{b}(\mathbf{x}) = [\mathbf{0}, \mathbf{M}_m^{-1}]^T$, $\mathbf{g} = [\mathbf{0}, -\mathbf{M}_m^{-1} \mathbf{G}_1]^T$, $\mathbf{d} = [\mathbf{0}, -\mathbf{M}_m^{-1} \mathbf{M}_1 \mathbf{M}_2^{-T} \mathbf{F}_2]^T$.

Due to external disturbances and parameters uncertainties, rewrite the dynamical model as below

$$\dot{\mathbf{x}} = \mathbf{f}_0(\mathbf{x}) + \mathbf{b}_0(\mathbf{x})\mathbf{u} + \boldsymbol{\omega} \quad (8)$$

$\mathbf{f}(\mathbf{x}) = \mathbf{f}_0(\mathbf{x}) + \Delta\mathbf{f}(\mathbf{x})$, $\mathbf{b}(\mathbf{x}) = \mathbf{b}_0(\mathbf{x}) + \Delta\mathbf{b}(\mathbf{x})$, $\boldsymbol{\omega} = \Delta\mathbf{f}(\mathbf{x}) + \Delta\mathbf{b}(\mathbf{x})\mathbf{u} + \mathbf{d}$ is bounded.

The control objectives of the system are to keep the object vertically and the gravity of the object is partly or completely compensated as demanded. When the reference input is given as $\mathbf{x}_{d1} = [l_d, 0, 0]^T$, then we have $\mathbf{x}_d = [\mathbf{x}_{d1}, \dot{\mathbf{x}}_{d1}]^T$, $\mathbf{e} = \mathbf{x} - \mathbf{x}_d$. Choose the sliding surface as Eq. (9).

$$\mathbf{s} = \boldsymbol{\psi}\mathbf{e} = 0 \tag{9}$$

where $\mathbf{s} = [s_1, s_2, s_3]^T \in \mathbf{R}^3$, $\boldsymbol{\alpha} = \text{diag}(\alpha_1, \alpha_2, \alpha_3)$, $\boldsymbol{\beta} = \text{diag}(\beta_1, \beta_2, \beta_3)$, $\boldsymbol{\psi} = [\boldsymbol{\alpha}, \boldsymbol{\beta}]^T$. The constant $\alpha_1, \alpha_2, \alpha_3, \beta_1, \beta_2, \beta_3$ and are chosen to be positive to make sure the relative polynomial is Hurwitz.

Theorem 1 For the AGOS (8), if the sliding function is defined as (9), the controller is designed as

$$\begin{aligned} \mathbf{u} = \mathbf{u}_e + \mathbf{u}_d, \mathbf{u}_e = & -(\boldsymbol{\psi}^T \mathbf{b}_0(\mathbf{x}))^{-1}(\boldsymbol{\psi}^T \mathbf{f}_0(\mathbf{x}) \\ & - \boldsymbol{\psi}^T \dot{\mathbf{x}}_d), \mathbf{u}_d = & -(\boldsymbol{\psi}^T \mathbf{b}_0(\mathbf{x}))^{-1} \text{diag}(\hat{\boldsymbol{\lambda}}) \text{sign}(\mathbf{s}) \end{aligned} \tag{10}$$

the sliding mode is guaranteed to be reached in finite time.

$\hat{\boldsymbol{\lambda}} = [\hat{\lambda}_1, \hat{\lambda}_2, \hat{\lambda}_3]^T$ is an adjustable parameter, and the adaptive law is

$$\dot{\hat{\boldsymbol{\lambda}}} = \left(\frac{1}{\rho_1} \|s_1\|, \frac{1}{\rho_2} \|s_2\|, \frac{1}{\rho_3} \|s_3\| \right)^T \tag{11}$$

where ρ_1, ρ_2, ρ_3 are positive.

Proof Assume that $\boldsymbol{\lambda}_d$ is the terminal solution of $\hat{\boldsymbol{\lambda}}$ which satisfies $\omega_1 < \lambda_{d1}, \omega_2 < \lambda_{d2}, \omega_3 < \lambda_{d3}$ respectively.

Choose the adaption error as:

$$\tilde{\boldsymbol{\lambda}} = \hat{\boldsymbol{\lambda}} - \boldsymbol{\lambda}_d \tag{12}$$

Consider a Lyapunov candidate function as:

$$V = \frac{1}{2} \mathbf{s}^T \mathbf{s} + \frac{1}{2} \tilde{\boldsymbol{\lambda}}^T \text{diag}(\rho_1, \rho_2, \rho_3) \tilde{\boldsymbol{\lambda}} \tag{13}$$

By differentiating V with respect to time, substituting Eqs. (9)–(12) into it, we have

$$\begin{aligned} \dot{V} &= \mathbf{s}^T (\boldsymbol{\psi}^T \mathbf{f}_0(\mathbf{x}) - \boldsymbol{\psi}^T \dot{\mathbf{x}}_d + \boldsymbol{\psi}^T \mathbf{b}_0(\mathbf{x}) \mathbf{u} + \boldsymbol{\omega}) + \tilde{\boldsymbol{\lambda}}^T \text{diag}(\rho_1, \rho_2, \rho_3) \dot{\tilde{\boldsymbol{\lambda}}} \\ &= \mathbf{s}^T (\boldsymbol{\omega} - \hat{\boldsymbol{\lambda}} \text{sign}(\mathbf{s})) + \tilde{\boldsymbol{\lambda}}^T \text{diag}(\rho_1, \rho_2, \rho_3) \dot{\tilde{\boldsymbol{\lambda}}} \\ &= s_1 \omega_1 + s_2 \omega_2 + s_3 \omega_3 - |s_1| \lambda_{d1} - |s_2| \lambda_{d2} - |s_3| \lambda_{d3} < 0 \end{aligned}$$

In order to reduce the input chattering caused by the $sign(s)$, the function $s./(|s| + \varepsilon)$ is used.

4 Simulation

The nominal values are $\hat{m}_1 = 0.5 \text{ kg}$, $\hat{m}_2 = 4 \text{ kg}$, $\hat{m}_{0x} = 16 \text{ kg}$, $\hat{m}_{0y} = 40 \text{ kg}$, $\hat{M} = 10 \text{ kg}$, $\hat{k} = 500 \text{ N/m}$, $\hat{l}_0 = 1 \text{ m}$, $\hat{g} = 10 \text{ m/s}^2$, $\hat{R} = 0.02 \text{ m}$. The parameter values are $m_1 = 0.55 \text{ kg}$, $m_2 = 4.4 \text{ kg}$, $m_{0x} = 17.6 \text{ kg}$, $m_{0y} = 44 \text{ kg}$, $M = 11 \text{ kg}$, $k = 550 \text{ N/m}$, $l_0 = 1.1 \text{ m}$, $g = 9.8 \text{ m/s}^2$, $R = 0.022 \text{ m}$.

The reference signals are given by $x_{d1} = [l_d, 0, 0]^T$ according to the simulation mechanism of AGFS and l_d represent offload quantity of the object gravity. When $l_d = 0$ the object's gravity is compensated completely and when $l_d = -0.2$ the object's gravity is at normal situation. When the value of l_d is between $(0, -0.2)$, the object's gravity is partly compensated and when l_d is positive, the object's gravity is greater than earth's gravity.

Fig. 3 shows the object driven inputs. For the control objectives we consider them as disturbances.

For the uncertain system with bounded disturbances and noises, the control parameters of the controller parameters are chosen as

$$\alpha = \text{diag}(120, 200, 200), \quad \beta = \text{diag}(2, 1, 1), \quad \rho_1 = 0.5, \rho_2 = \rho_3 = 1, \\ \hat{\lambda}_0 = [80, 10, 10]^T$$

The boundary layer $\|s\| \leq 6.2 \times 10^{-3}$ is reached in the finite time and the settling time $t \leq 0.3 \text{ s}$ and $\|e\| \leq 2.0 \times 10^{-4}$ as shown in Figs. 4 and 5.

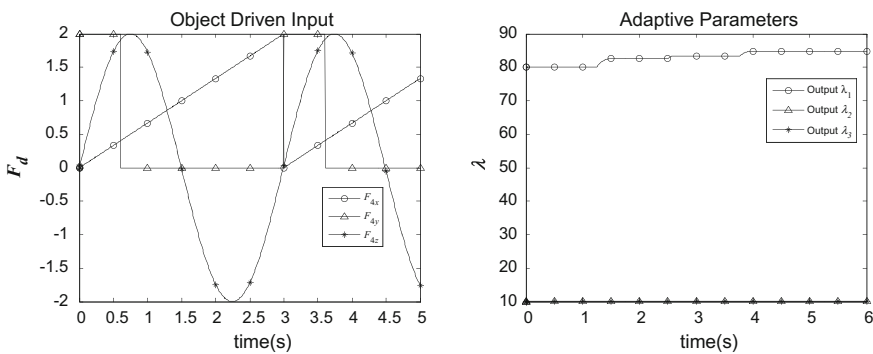


Fig. 3 The object driven input and adaptive parameters $\hat{\lambda}$

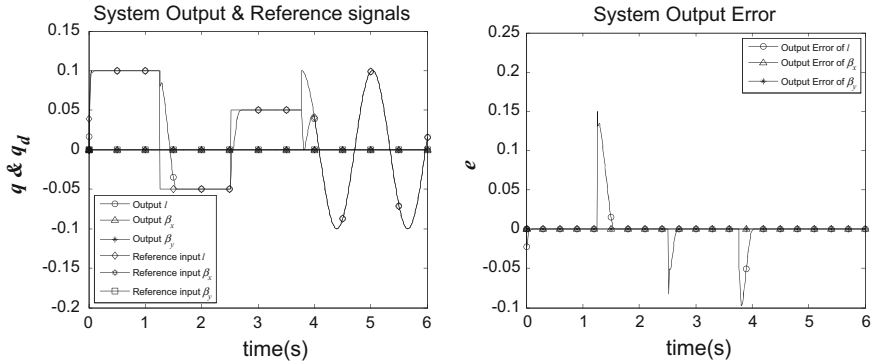


Fig. 4 The system outputs and reference inputs, system output errors

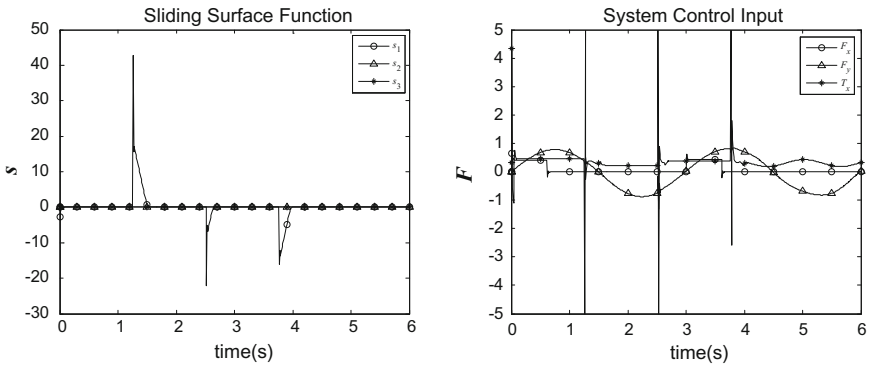


Fig. 5 The sliding surfaces and system control inputs

5 Conclusions

In this paper, an active gravity offload system is introduced in details. It's a servo platform consisting of a suspension structure, a buffer, a universal joint, a gantry robot, a tilt sensor and a tension sensor. A variable gravity field is built by the gravity offload system with the adaptive sliding mode controller.

Acknowledgment This work was supported by the NSFC (61327807, 61521091, 61520106010, 61134005) and the National Basic Research Program of China (973 Program: 2012CB821200, 2012CB821201).

References

1. Watanabe Y (1988) Microgravity experiments for a visual feedback control of a space robot capturing a target. In: International conference on IEEE, vol 3, pp 1993–1998
2. Sawada H (2004) Micro-gravity experiment of a space robotic arm using parabolic flight. *Adv Robot* 18(3):247–267
3. Menon C (2007) Issues and solutions for testing free-flying robots. *Acta Astronaut* 60(12): 957–965
4. Robertson A (1999) Spacecraft formation flying control design for the Orion mission. In: AIAA guidance, navigation, and control conference, pp 1562–1575
5. Kienholz AD (1989) Very low frequency suspension systems for dynamic testing. In: Proceedings of the 30th structures, structural dynamics and materials, pp 327–336
6. White GC (1994) Active vertical-direction gravity compensation system. *IEEE Trans Instrum Meas* 43(6):786–792
7. Han O (2010) Gravity-offloading system for large-displacement ground testing of spacecraft mechanisms. In: Proceedings of 40th aerospace mechanisms symposium, pp 119–132
8. Huang YJ (2008) Adaptive sliding-mode control for nonlinear systems with uncertain parameters. *IEEE Trans Syst Man Cybern* 38(2):534–539
9. Duan M (2016) Adaptive sliding mode control for A 2 DOF magnetic levitation system with uncertain parameters. *J Rob Networking Artif Life* 2(4):263–267